Available online at www.sciencedirect.com
ScienceDirect
Nuclear Physics A 866 (2011) 1–15
NUCLEAR PHYSICS A
www.elsevier.com/locate/nuclphysa

α-Decay near the shell closure from ground and isomeric states

Yibin Qian [a,*], Zhongzhou Ren [a,b,c], Dongdong Ni [a]

[a] *Department of Physics, Nanjing University, Nanjing 210093, China*
[b] *Center of Theoretical Nuclear Physics, National Laboratory of Heavy-Ion Accelerator, Lanzhou 730000, China*
[c] *Kavli Institute for Theoretical Physics China, Beijing 100190, China*

Received 3 June 2011; accepted 7 July 2011

Available online 19 July 2011

Abstract

The modified two-potential approach (MTPA) is employed to study the exotic α-decay near the closed shells $Z = 82$ and $N = 82$, 126 within a deformed version of the cluster model. We perform systematic calculations on favored α-decay half-lives from both the ground states (g.s.) and the isomeric states (i.s.) by using the microscopic double-folding potential. The obtained α-decay half-lives are found to be in good agreement with the experimental data. This indicates that four types of α transitions among ground states and isomeric states (g.s. $\rightarrow$ g.s., g.s. $\rightarrow$ i.s., i.s. $\rightarrow$ g.s., i.s. $\rightarrow$ i.s.) are well described in a unified model. In addition, the unfavored α transitions in the Bi isotopes are investigated to pursue a further understanding of α-decay properties.

Keywords: α-Decay; Half-lives; Cluster model

1. Introduction

The discovery of unknown radiation by Becquerel one century ago, can be taken as the prelude of the study on α-decay. Before long, α-decay was firstly observed in the experiment by Rutherford and Geiger in 1908 [1]. α-Decay, as one of the most important decay modes for unstable nuclei, has long been a realistic and precise probe to study nuclear structure properties [2–7]. Moreover, it is a reliable method to identify new element and new isomeric states

* Corresponding author. Tel.: +86 025 83596499; fax: +86 025 83326028.
E-mail address: qyibin@gmail.com (Y. Qian).

0375-9474/$ – see front matter
doi:10.1016/j.nuclphysa.2011.07.002

[8–11], via the observation of α-decay chains from unknown parent nuclei to known nuclei. Very recently, the 117th superheavy element has been synthesized in the fusion reaction using ^{249}Bk targets with ^{48}Ca beams, filling the final gap of the element chart up to $Z = 118$ [11]. From the theoretical side, Gamow [12] and Condon and Gurney [13] independently described α-decay as a consequence of the quantum tunneling for the first time in 1928. This theoretical work was the pioneering application of quantum mechanics to nuclear physics. Up to now, based on various models like the cluster model, the shell model and the fissionlike model, many effective approaches such as GLDM [14,15], GDDCM [16], DDCM [17], UMADAC [18], CPPMDN [19], the coupled-channel approach [20–22] have been proposed to evaluate the absolute α-decay width. Recently, several analytical expressions for α-decay half-lives have also been proposed with phenomenological methods, including some important ingredients like the shell effect, the angular momentum and parity carried by the α-particle [23–27].

α Transitions usually take place from g.s. to g.s., with the same angular momenta and parities. These favored α-decays are the primary pattern of all even–even nuclei and parts of odd-A and odd–odd nuclei. Due to the strong hindrance caused by the nonzero momentum of the α-particle, α transitions of odd-A and odd–odd nuclei around the proton and neutron shells, may choose to decay from or to isomeric states [28]. Such α-decays may provide valuable information on the structure properties of exotic nuclei near the shell closures. Experimentally, a lot of α-decay data have been accumulated in the region near the closed shell $N = 82$ and $Z = 82$ for neutron-deficient nuclei [29–34], e.g., detailed α-decay studies of Tl, Pb, Bi, and At isotopes [33,34]. Moreover, there is also the attempt to search for unknown neutron-deficient nuclei, related to the effects of the shell $N = 126$, in the heavy nuclei region [35]. These can be considered as an encouragement for us to investigate the interesting α-decays in the closed-shell region.

As a fully quantum method based on the perturbation theory, the two-potential approach (TPA) not only provides good physical insights but it is simple and accurate as well [36,37]. Moreover, Gurvitz et al. have proposed further developments for TPA, representing the corrections to TPA. And they also demonstrate that, without losing its accuracy, the TPA can be induced to a modified form resembling the R-matrix theory, yet without the uncertainties related to the choice of the matching radius [37]. Recently, we have employed the spherical version of this MTPA to evaluate α-decay half-lives [38,39], and have also extended the MTPA for a deformed system to study heavy and superheavy nuclei [40]. The numerical results in the previous calculations are found to agree well with the experimental data. As for many α-decay calculations, our previous studies are concentrated on the ground-states-to-ground-states α transitions of even–even nuclei and a few odd-A and odd–odd nuclei. Meanwhile, although the experiments have already provided a wealth of α-decay data in ground and isomeric states of neutron-deficient nuclei, theoretical studies on them are comparatively rare. As further extension and test of our work, we have performed a detailed study of α transitions from ground and isomeric states of these odd-A and odd–odd nuclei, in the present study. The MTPA within a deformed version of the cluster model is used to give a description of α-decay, where the α-nucleus potential is obtained by the microscopic double-folding method. To obtain the α-decay width, the numerical solution of the radial Schrödinger equation for the bound state, along with the Wildermuth rule [41], is presented.

This article is organized as follows. In Section 2, a brief description of the theoretical framework is shown for the calculation of α-decay half-lives. In Section 3, numerical results and detailed discussions on the α transitions from both ground and isomeric states are presented. A brief summary is given in Section 4.

2. Theoretical framework

The two-potential approach (TPA) can consistently achieve a goal that a tunneling problem is essentially simplified by reducing it to two separate problems: a bound state problem and a scattering state problem [36,37]. By a separation radius R, this approach represents the barrier potential $V(r)$ as a sum of the "inner" term and the "outer" term. The original version of TPA is served for one-dimensional (1D) or spherical cases. To extend the α-decay width for deformed nuclei, we assume an α particle interacts with an axially symmetric deformed daughter nucleus. Based on the popular M3Y-Reid-type nucleon–nucleon interaction and the standard Coulomb proton–proton interaction, the nuclear and Coulomb potentials can be obtained in the double folding model:

$$V_{N\,or\,C}(r,\theta) = \iint d\mathbf{r}_1\, d\mathbf{r}_2\, \rho_1(\mathbf{r}_1)\upsilon\big(\mathbf{s} = |\mathbf{r}_2 + \mathbf{r} - \mathbf{r}_1|\big)\rho_2(\mathbf{r}_2), \tag{1}$$

where θ is the orientation angle of the emitted α-particle with respect to the symmetric axis of the deformed daughter nucleus, $\upsilon(\mathbf{s})$ is the effective nucleon–nucleon interaction. The density distribution of the spherical α particle ρ_1 is described as a standard Gaussian form [42]. And ρ_2 is a deformed Fermi distribution of the core nucleus, which is given by:

$$\rho_2(r_2,\theta) = \frac{\rho_0}{1 + \exp[\frac{r_2 - R(\theta)}{a}]}, \tag{2}$$

where the ρ_0 value is fixed by integrating the density distribution equivalent to the mass and proton numbers of the daughter nucleus, respectively, for the nuclear and Coulomb potentials. The half-density radius $R(\theta) = R_0[1 + \beta_2 Y_{20}(\theta) + \beta_4 Y_{40}(\theta)]$, $R_0 = 1.07A_d^{1/3}$ fm, diffuseness $a = 0.54$ fm (see Refs. [17,22] and references therein). For the spherical-deformed interacting system, the double folding potential is numerically achieved by using the multipole expansion. The details on the evaluation of the potential and the effective interaction can be found in Refs. [42,43,17,22]. Then the total interaction potential, including the attractive part, the repulsive Coulomb part and the additional centrifugal part, is given by:

$$V(r,\theta) = \lambda V_N(r,\theta) + V_C(r,\theta) + \frac{\hbar^2\ell(\ell+1)}{2\mu r^2}, \tag{3}$$

where λ is the renormalization factor, i.e., the depth of the nuclear potential, ℓ is the angular momentum carried by the α particle, and μ is the reduced mass of the α-core system. For one certain orientation angle θ, the total potential $V(r,\theta)$ can be reduced to $V(r)$, similar to the 1D or spherical case. According to the MTPA, one can introduce two auxiliary potentials [36,37]: the inner potential

$$U(r) = \begin{cases} V(r), & r \leqslant R, \quad (4a) \\ V(R) = V_0, & r > R, \quad (4b) \end{cases}$$

and the outer potential

$$\tilde{W}(r) = \begin{cases} V_0, & r \leqslant R, \quad (5a) \\ V(r), & r > R. \quad (5b) \end{cases}$$

The separation radius R, related to the corrections to TPA, is taken reasonably inside the barrier of $V(r)$ [37]. Note that the "shifted" potential $\tilde{W}(r)$, vanishing for $r \to \infty$, is introduced to solve the eigenproblem perturbatively in the TPA [36].

In the following way, we numerically solve the radial Schrödinger equation within the inner potential U for the bound solution $\phi_{n\ell j}(r)$, which vanishes gradually in an exponential type from the separation radius R [40]. The renormalization factor λ is adjusted to make the bound-state wave function characterized by the experimental Q_α value and the special quantum number determined by the Wildermuth condition [41], which is given by

$$G = 2n + \ell = \sum_{i=1}^{4} g_i. \tag{6}$$

In the above expression, n is the number of internal nodes in the radial wave function, and g_i is the corresponding oscillator quantum numbers of the nucleons composing the α cluster. These g values, restricted by the Pauli principle, are chosen to guarantee the α cluster outside the shell occupied entirely by the daughter nucleus. It should be noted that a zero-potential term for the single-nucleon exchange, in the M3Y interaction, guarantees the antisymmetrization of identical nucleons in the α cluster and the daughter nucleus [16,42,43]. Once the wavefunction $\phi_{n\ell j}(r)$ is solved following the above procedure, one can obtain the decay width in the MTPA, for a certain angle θ:

$$\Gamma(\theta) = \frac{\hbar^2 k}{\mu}\left[\frac{\phi_{n\ell j}(\bar{r})}{G_\ell(k\bar{r})}\right]^2. \tag{7}$$

Here $k = \sqrt{2\mu Q_\alpha}/\hbar$, and G_ℓ is the irregular Coulomb wave function. The value of $\bar{r}$ is chosen in such a way that the potential $V(r)$ can be well approximated by the repulsive part (i.e. the attractive part disregards) for $r \geqslant \bar{r}$. As discussed in Refs. [36,37], the decay width $\Gamma(\theta)$ does not depend on the particular choice of R or $\bar{r}$.

Following the average procedure widely applied for a deformed α-core system [17–19,40,44], the final α-decay width can be obtained by averaging it in all directions:

$$\Gamma = \int_0^{\pi/2} \Gamma(\theta)\sin(\theta)\,d\theta. \tag{8}$$

Then the half-life of α-decay is related to the decay width by

$$T_{1/2} = \frac{\hbar \ln 2}{P_\alpha \Gamma}, \tag{9}$$

where the indispensable quantity P_α is the preformation factor. Considering that α-decay is a rich resource of nuclear structure information, the P_α value is very important in terms of the nuclear structure. Several approaches have been proposed to obtain this quantity [6], e.g., combining the shell model with the BCS method [45], and supplementing the shell model wavefunction with a cluster component (i.e. the hybrid model) [46]. Nevertheless, it is quite difficult to evaluate the P_α value due to the complexity of both the nuclear potential and the nuclear many-body problem. By now, there is just a typical example for the typical nucleus ^{212}Po with two protons and two neutrons outside the double magic shell based on the hybrid model, which indicates that the weight of clustering is as high as 0.3 [46]. Experimentally, it is shown that the preformation factor varies smoothly in the open shell region and has a value smaller than 1 [6]. Consequently, it is appropriate to take the preformation factor as the same constant for one kind of nuclei. In this study, its value is taken as the following: $P_\alpha = 0.38$ for even–even nuclei, $P_\alpha = 0.27$ for odd-A nuclei, and $P_\alpha = 0.17$ for odd–odd nuclei. These values are consistent with our previous

calculations [39,40], and agree well with both the theoretical calculation for ^{212}Po [46] and the analysis from the experiments [6]. Moreover, it is reasonable to take above P_α values in order, respectively, for even–even, odd-A and odd–odd nuclei, due to the block effect of odd nucleons.

3. Numerical results and discussions

We have firstly performed a systematic calculation on the favored α transitions from both the g.s. and i.s. near the shells $Z = 82$ and $N = 82, 126$, by using the MTPA for the deformed α-core system. The experimental values, such as decay energies and half-lives, are mainly taken from Refs. [47,48], and some recent data are from Refs. [16,34,49,50] and references therein. Besides, the deformation parameters used in the calculations are mostly taken from Möller et al. [51]. In these α-decays, a parent nucleus and the corresponding daughter nucleus have the same spins and parities. Considering that the emitted α particle obeys the spin-parity selection rule [18,19], the angular momentum and parity of the α particle is taken as 0^+ (i.e. favored α transition). In fact, because of the strong hindrance of the additional centrifugal potential ($\ell \neq 0$), branching ratios of the α transitions with nonzero angular momentum are very small as compared to those of favored transitions.

The detailed numerical results and the experimental data on α transitions near the magic shells $N = 82$, 126 and $Z = 82$ are, respectively, listed in Tables 1, 3 and Table 2. In these tables, the first column denotes α transitions from parent nuclei to corresponding daughter nuclei. The superscript "m", "n", "p" on nuclide names denote the first, second, third isomeric states respectively. The second column shows the transition of the spin and parity from a parent nucleus to the corresponding daughter nucleus ($I_i^\pi \to I_j^\pi$). The decay energies Q_α, experimental α-decay half-lives, and computed half-lives are presented in the last three columns, respectively. The

Table 1
Comparison of the experimental and calculated half-lives for α-decays from ground and isomeric states near the neutron shell $N = 82$. The symbol # indicates the tentative assignment from Refs. [47,48].

α transition	$I_i^\pi \to I_j^\pi$	N	Q_α (MeV)	$T_{1/2}^{expt}$ (s)	$T_{1/2}^{calc}$ (s)
^{151}Ho $\to$ ^{147}Tb^m	$11/2^- \to 11/2^-$	84	4.640	1.60×10^2	1.48×10^2
^{151}Ho^m $\to$ ^{147}Tb	$1/2^+ \to 1/2^+$	84	4.729	5.90×10^1	5.04×10^1
^{153}Tm $\to$ ^{149}Ho	$11/2^- \to 11/2^-$	84	5.240	1.63×10^0	1.90×10^0
^{153}Tm^m $\to$ ^{149}Ho^m	$1/2^+ \to 1/2^+$	84	5.233	2.69×10^0	2.05×10^0
^{155}Lu $\to$ ^{151}Tm	$11/2^- \to 11/2^-$	84	5.803	7.56×10^{-2}	7.26×10^{-2}
^{155}Lu^m $\to$ ^{151}Tm^m	$1/2^+ \to 1/2^+$	84	5.729	1.82×10^{-1}	1.45×10^{-1}
^{157}Ta $\to$ ^{153}Lu^m	$1/2^+ \to 1/2^+$	84	6.275	1.05×10^{-2}	9.65×10^{-3}
^{157}Ta^m $\to$ ^{153}Lu	$11/2^- \to 11/2^-$	84	6.377	4.30×10^{-3}	4.11×10^{-3}
^{151}Dy $\to$ ^{147}Gd	$7/2^- \to 7/2^-$	85	4.180	1.92×10^4	1.66×10^4
^{152}Ho $\to$ ^{148}Tb	$2^- \to 2^-$	85	4.507	1.35×10^3	1.24×10^3
^{152}Ho^m $\to$ ^{148}Tb^m	$2^- \to 2^-$	85	4.577	4.58×10^2	5.09×10^2
^{153}Er $\to$ ^{149}Dy	$7/2^- \to 7/2^-$	85	4.802	7.00×10^1	7.13×10^1
^{154}Tm $\to$ ^{150}Ho	$2^- \to 2^-$	85	5.094	1.50×10^1	1.44×10^1
^{154}Tm^m $\to$ ^{150}Ho^m	$9^+ \to 9^+$	85	5.175	5.69×10^0	5.95×10^0
^{155}Yb $\to$ ^{151}Er	$7/2^- \to 7/2^-$	85	5.338	2.02×10^0	3.50×10^0
^{156}Lu $\to$ ^{152}Tm	$2^- \to 2^-$	85	5.597	4.94×10^{-1}	8.14×10^{-1}

(*continued on next page*)

Table 1 (*continued*)

α transition	$I_i^\pi \to I_j^\pi$	N	Q_α (MeV)	$T_{1/2}^{expt}$ (s)	$T_{1/2}^{calc}$ (s)
$^{156}Lu^m \to {}^{152}Tm^m$	$9^+ \to 9^+$	85	5.711	2.02×10^{-1}	2.69×10^{-1}
$^{157}Hf \to {}^{153}Yb$	$7/2^- \to 7/2^-$	85	5.880	1.17×10^{-1}	1.02×10^{-1}
$^{158}Ta \to {}^{154}Lu$	$2^- \to 2^-$	85	6.123	7.20×10^{-2}	5.60×10^{-2}
$^{158}Ta^m \to {}^{154}Lu^m$	$9^+ \to 9^+$	85	6.205	3.77×10^{-2}	2.74×10^{-2}
$^{159}W \to {}^{155}Hf$	$7/2^- \to 7/2^-$	85	6.457	8.24×10^{-3}	9.39×10^{-3}
$^{160}Re \to {}^{156}Ta$	$2^- \to 2^-$	85	6.708	8.78×10^{-3}	3.47×10^{-3}
$^{153}Ho \to {}^{149}Tb^m$	$11/2^- \to 11/2^-$	86	4.015	2.36×10^{6}	7.39×10^{6}
$^{153}Ho^m \to {}^{149}Tb$	$1/2^+ \to 1/2^+$	86	4.119	3.10×10^{5}	1.51×10^{5}
$^{155}Tm \to {}^{151}Ho$	$11/2^- \to 11/2^-$	86	4.572	2.43×10^{3}	4.40×10^{3}
$^{155}Tm^m \to {}^{151}Ho^m$	$1/2^+ \to 1/2^+$	86	4.572	$> 2.25 \times 10^{3}$	4.40×10^{3}
$^{157}Lu \to {}^{153}Tm^m$	$11/2^- \to 11/2^-$	86	5.054	1.23×10^{2}	1.38×10^{2}
$^{157}Lu^m \to {}^{153}Tm$	$1/2^+ \to 1/2^+$	86	5.129	7.98×10^{1}	6.73×10^{1}
$^{159}Ta \to {}^{155}Lu^m$	$1/2^+ \to 1/2^+$	86	5.661	2.44×10^{0}	2.49×10^{0}
$^{159}Ta^m \to {}^{155}Lu$	$11/2^- \to 11/2^-$	86	5.745	9.09×10^{-1}	1.09×10^{0}
$^{153}Dy \to {}^{149}Gd$	$7/2^- \to 7/2^-$	87	3.559	2.45×10^{8}	3.14×10^{8}
$^{154}Ho \to {}^{150}Tb$	$2^- \to 2^-$	87	< 4.042	3.71×10^{6}	$> 6.89 \times 10^{5}$
$^{154}Ho^m \to {}^{150}Tb^m$	$8^+ \to 8^+$	87	3.820	$> 1.86 \times 10^{7}$	2.36×10^{7}
$^{155}Er \to {}^{151}Dy$	$7/2^- \to 7/2^-$	87	4.118	1.45×10^{6}	5.87×10^{5}
$^{156}Tm \to {}^{152}Ho$	$2^- \to 2^-$	87	4.343	1.31×10^{5}	1.40×10^{5}
$^{157}Yb \to {}^{153}Er$	$7/2^- \to 7/2^-$	87	4.621	7.72×10^{3}	8.01×10^{3}
$^{158}Lu \to {}^{154}Tm$	$2^- \to 2^-$	87	4.790	1.16×10^{3}	3.06×10^{3}
$^{159}Hf \to {}^{155}Yb$	$7/2^- \to 7/2^-$	87	5.225	3.25×10^{1}	4.22×10^{1}
$^{160}Ta \to {}^{156}Lu$	$2^- \to 2^-$	87	5.449	$\geqslant 1.70 \times 10^{0}$	3.27×10^{1}
$^{160}Ta^m \to {}^{156}Lu^m$	$9^+ \to 9^+$	87	5.552	4.56×10^{0}	1.12×10^{1}
$^{161}W \to {}^{157}Hf$	$7/2^-\# \to 7/2^-$	87	5.923	4.77×10^{-1}	5.81×10^{-1}
$^{162}Re \to {}^{158}Ta$	$2^- \to 2^-$	87	6.240	1.14×10^{-1}	1.53×10^{-1}
$^{162}Re^m \to {}^{158}Ta^m$	$9^+ \to 9^+$	87	6.274	9.00×10^{-2}	1.14×10^{-1}
$^{163}Os \to {}^{159}W$	$7/2^-\# \to 7/2^-\#$	87	6.677	5.61×10^{-3}	7.00×10^{-3}

difference of these three tables is that the third column, respectively, displays the neutron number and the proton number for Tables 1, 3 and Table 2. There are four types of favored α transitions in this study: (1) from ground states to ground states, (2) from ground states to isomeric states, (3) from isomeric states to ground states, (4) from isomeric states to isomeric states. As shown in the tables, the numerical α-decay half-lives agree well with measured data, although the α-decay half-lives span a large order of magnitude. Some new data (or measured with improved accuracy) of α transitions from the parent nuclei such as $^{179}Tl^m$, ^{179}Pb, ^{180}Pb, ^{187}Po, and ^{188}Po, are also well reproduced by the present calculations. This means that the MTPA for deformed nuclei, is valid for α-decays from both ground and isomeric states.

From the tables, one can see that the α-decay half-lives of isomeric states are comparable to those of ground states, and some of them are even longer than those of the corresponding ground states. It is obvious that the experimental α-decay lifetimes are well reproduced for both g.s. and i.s., and the P_α values, no matter from the g.s. or i.s., are chosen as identical ones. As a

Table 2
Same as Table 1 but for parent nuclei around the proton shell $Z = 82$, including some new data in the recent experiments (denoted by $*$).

α transition	$I_i^\pi \to I_j^\pi$	Z	Q_α (MeV)	$T_{1/2}^{expt}$ (s)	$T_{1/2}^{calc}$ (s)
$^{177}\mathrm{Tl} \to {}^{173}\mathrm{Au}$	$1/2^+ \to 1/2^+$	81	7.067	2.47×10^{-2}	3.28×10^{-2}
$^{177}\mathrm{Tl}^m \to {}^{173}\mathrm{Au}^m$	$11/2^- \to 11/2^-$	81	7.660	4.69×10^{-4}	4.06×10^{-4}
$^{179}\mathrm{Tl} \to {}^{175}\mathrm{Au}$	$1/2^+ \to 1/2^+$	81	6.719	2.30×10^{-1}	5.15×10^{-1}
$*{}^{179}\mathrm{Tl}^m \to {}^{175}\mathrm{Au}^m$	$11/2^- \to 11/2^-$	81	7.378	2.25×10^{-3}	2.80×10^{-3}
$^{181}\mathrm{Tl} \to {}^{177}\mathrm{Au}$	$1/2^+ \to 1/2^+$	81	6.321	$> 3.20 \times 10^{1}$	1.66×10^{1}
$^{181}\mathrm{Tl}^m \to {}^{177}\mathrm{Au}^m$	$9/2^- \to 9/2^-$	81	6.727	3.65×10^{-1}	4.43×10^{-1}
$^{183}\mathrm{Tl}^m \to {}^{179}\mathrm{Au}^m$	$9/2^- \to 9/2^-$	81	6.479	4.28×10^{0}	3.57×10^{0}
$^{185}\mathrm{Tl}^m \to {}^{181}\mathrm{Au}^m$	$9/2^- \to 9/2^-$	81	6.108	$\approx 1.18 \times 10^{2}$	1.09×10^{2}
$*{}^{179}\mathrm{Pb} \to {}^{175}\mathrm{Hg}^m$	$(9/2^-) \to (9/2^-)$	82	7.518	3.50×10^{-3}	2.75×10^{-3}
$*{}^{180}\mathrm{Pb} \to {}^{176}\mathrm{Hg}^m$	$0^+ \to 0^+$	82	7.419	4.00×10^{-3}	3.88×10^{-3}
$*{}^{181}\mathrm{Pb} \to {}^{177}\mathrm{Hg}^m$	$(9/2^-) \to (9/2^-)$	82	7.175	3.60×10^{-2}	3.36×10^{-2}
$^{183}\mathrm{Pb} \to {}^{179}\mathrm{Hg}^m$	$(3/2^-) \to (3/2^-)$	82	6.723	2.20×10^{0}	1.38×10^{0}
$^{183}\mathrm{Pb}^m \to {}^{179}\mathrm{Hg}^n$	$(13/2^+) \to (13/2^+)$	82	6.854	4.25×10^{-1}	4.09×10^{-1}
$^{185}\mathrm{Pb} \to {}^{181}\mathrm{Hg}^m$	$3/2^- \to 3/2^-$	82	6.629	4.20×10^{1}	2.64×10^{0}
$^{185}\mathrm{Pb} \to {}^{181}\mathrm{Hg}^n$	$3/2^- \to 3/2^-$	82	6.427	3.31×10^{1}	1.64×10^{1}
$^{185}\mathrm{Pb}^m \to {}^{181}\mathrm{Hg}^p$	$13/2^+ \to 13/2^+$	82	6.550	8.14×10^{0}	5.33×10^{0}
$^{187}\mathrm{Pb} \to {}^{183}\mathrm{Hg}^m$	$(3/2^-) \to (3/2^-)$	82	6.329	3.62×10^{2}	3.82×10^{1}
$^{187}\mathrm{Pb} \to {}^{183}\mathrm{Hg}^n$	$(3/2^-) \to (3/2^-)$	82	6.124	5.39×10^{2}	2.88×10^{2}
$^{187}\mathrm{Pb}^m \to {}^{183}\mathrm{Hg}^p$	$(13/2^+) \to (13/2^+)$	82	6.210	1.53×10^{2}	1.19×10^{2}
$^{191}\mathrm{Pb} \to {}^{187}\mathrm{Hg}$	$3/2^- \to 3/2^-$	82	5.403	6.14×10^{5}	6.57×10^{5}
$^{186}\mathrm{Bi} \to {}^{182}\mathrm{Tl}^m$	$3^+ \to 3^+\#$	83	7.309	1.48×10^{-2}	4.58×10^{-2}
$^{186}\mathrm{Bi}^m \to {}^{182}\mathrm{Tl}^n$	$10^- \to 10^-$	83	7.423	9.8×10^{-3}	1.11×10^{-2}
$^{187}\mathrm{Bi} \to {}^{183}\mathrm{Tl}^m$	$9/2^- \to 9/2^-$	83	7.147	4.02×10^{-2}	9.68×10^{-2}
$^{187}\mathrm{Bi}^m \to {}^{183}\mathrm{Tl}$	$1/2^+ \to 1/2^+$	83	7.883	3.10×10^{-4}	4.40×10^{-4}
$^{188}\mathrm{Bi}^m \to {}^{184}\mathrm{Tl}^m$	$3^+ \to 3^+$	83	7.144	6.00×10^{-2}	1.55×10^{-1}
$^{188}\mathrm{Bi}^n \to {}^{184}\mathrm{Tl}^n$	$10^- \to 10^-$	83	6.961	2.91×10^{-1}	6.82×10^{-1}
$^{189}\mathrm{Bi} \to {}^{185}\mathrm{Tl}^m$	$9/2^- \to 9/2^-$	83	6.815	9.51×10^{-1}	1.41×10^{0}
$^{189}\mathrm{Bi}^m \to {}^{185}\mathrm{Tl}$	$1/2^+ \to 1/2^+$	83	7.455	6.85×10^{-3}	4.75×10^{-3}
$^{190}\mathrm{Bi}^m \to {}^{186}\mathrm{Tl}^m$	$3^+ \to 3^+$	83	6.569	7.33×10^{0}	1.07×10^{1}
$^{190}\mathrm{Bi}^n \to {}^{186}\mathrm{Tl}^n$	$10^- \to 10^-$	83	6.595	9.25×10^{0}	1.49×10^{1}
$^{191}\mathrm{Bi} \to {}^{187}\mathrm{Tl}^m$	$9/2^- \to 9/2^-$	83	6.443	2.43×10^{1}	3.56×10^{1}
$^{191}\mathrm{Bi}^m \to {}^{187}\mathrm{Tl}$	$1/2^+ \to 1/2^+$	83	7.017	1.78×10^{-1}	1.44×10^{-1}
$^{192}\mathrm{Bi} \to {}^{188}\mathrm{Tl}^m$	$3^+ \to 3^+$	83	6.189	2.97×10^{2}	6.47×10^{2}
$^{192}\mathrm{Bi}^m \to {}^{188}\mathrm{Tl}^n$	$10^- \to 10^-$	83	6.181	4.37×10^{2}	7.06×10^{2}
$^{193}\mathrm{Bi} \to {}^{189}\mathrm{Tl}^m$	$9/2^- \to 9/2^-$	83	6.024	2.00×10^{3}	2.13×10^{3}
$^{193}\mathrm{Bi}^m \to {}^{189}\mathrm{Tl}$	$1/2^+ \to 1/2^+$	83	6.612	3.81×10^{0}	4.15×10^{0}
$^{194}\mathrm{Bi} \to {}^{190}\mathrm{Tl}^m$	$3^+ \to 3^+$	83	5.764	2.08×10^{4}	5.31×10^{4}
$^{194}\mathrm{Bi}^m \to {}^{190}\mathrm{Tl}^n$	$10^- \to 10^-$	83	5.717	6.28×10^{4}	8.98×10^{4}
$^{195}\mathrm{Bi} \to {}^{191}\mathrm{Tl}^m$	$9/2^- \to 9/2^-$	83	5.534	6.10×10^{5}	4.54×10^{5}

(*continued on next page*)

α transition	$I_i^\pi \to I_j^\pi$	Z	Q_α (MeV)	$T_{1/2}^{expt}$ (s)	$T_{1/2}^{calc}$ (s)
^{195}Bi$^m \to ^{191}$Tl	$1/2^+ \to 1/2^+$	83	6.234	2.64×10^2	2.28×10^2
^{196}Bi $\to ^{192}$Tl^m	$3^+ \to 3^+$	83	5.260	2.68×10^7	2.02×10^7
^{196}Bi$^m \to ^{192}$Tl^n	$10^- \to 10^-$	83	5.219	6.32×10^7	3.42×10^7
$*^{187}$Po $\to ^{183}$Pb^m	$(1/2, 5/2)^- \to (1/2, 5/2)^-$	84	7.693	1.40×10^{-3}	2.50×10^{-3}
$*^{188}$Po $\to ^{184}$Pb	$0^+ \to 0^+$	84	8.082	2.70×10^{-4}	1.12×10^{-4}
^{191}Po $\to ^{187}$Pb^m	$3/2^- \to 3/2^-$	84	7.491	2.85×10^{-2}	9.63×10^{-3}
^{191}Po$^m \to ^{187}$Pb^n	$13/2^+ \to 13/2^+$	84	7.035	2.55×10^{-1}	3.41×10^{-1}
$*^{192}$Po $\to ^{188}$Pb	$0^+ \to 0^+$	84	7.319	3.23×10^{-2}	2.42×10^{-2}
^{193}Po $\to ^{189}$Pb	$3/2^- \to 3/2^-$	84	7.095	4.20×10^{-1}	1.95×10^{-1}
^{193}Po$^m \to ^{189}$Pb^m	$13/2^+ \to 13/2^+$	84	7.150	2.40×10^{-1}	1.25×10^{-1}
^{195}Po $\to ^{191}$Pb	$3/2^- \to 3/2^-$	84	6.747	6.19×10^0	3.48×10^0
^{195}Po$^m \to ^{191}$Pb^m	$13/2^+ \to 13/2^+$	84	6.839	2.13×10^0	1.55×10^0
^{197}Po $\to ^{193}$Pb	$3/2^- \to 3/2^-$	84	6.412	1.27×10^2	7.04×10^1
^{197}Po$^m \to ^{193}$Pb^m	$13/2^+ \to 13/2^+$	84	6.515	3.10×10^1	2.63×10^1
^{199}Po $\to ^{195}$Pb	$3/2^- \to 3/2^-$	84	6.074	2.74×10^3	1.86×10^3
^{199}Po$^m \to ^{195}$Pb^m	$13/2^+ \to 13/2^+$	84	6.183	6.42×10^2	6.07×10^2
^{201}Po $\to ^{197}$Pb	$3/2^- \to 3/2^-$	84	5.798	5.74×10^4	3.38×10^4
^{201}Po$^m \to ^{197}$Pb^m	$13/2^+ \to 13/2^+$	84	5.903	1.84×10^4	1.07×10^4
^{203}Po $\to ^{199}$Pb^m	$5/2^- \to 5/2^-$	84	5.491	2.00×10^6	1.12×10^6
^{205}Po $\to ^{201}$Pb	$5/2^- \to 5/2^-$	84	5.324	1.57×10^7	8.33×10^6
^{207}Po $\to ^{203}$Pb	$5/2^- \to 5/2^-$	84	5.216	9.94×10^7	3.15×10^7
^{191}At $\to ^{187}$Bi^m	$1/2^+ \to 1/2^+$	85	7.714	1.70×10^{-3}	4.78×10^{-3}
^{191}At$^m \to ^{187}$Bi^n	$7/2^- \to 7/2^-$	85	7.817	2.14×10^{-3}	2.30×10^{-3}
^{192}At$^m \to ^{188}$Bi^m		85	7.593	2.05×10^{-2}	1.78×10^{-2}
^{192}At$^n \to ^{188}$Bi^n	$(9, 10)^- \to (9, 10)^-$	85	7.378	1.07×10^{-1}	9.09×10^{-2}
^{193}At $\to ^{189}$Bi^m	$1/2^+ \to 1/2^+$	85	7.388	2.80×10^{-2}	5.11×10^{-2}
^{193}At$^m \to ^{189}$Bi^n	$7/2^- \to 7/2^-$	85	7.480	2.14×10^{-2}	2.53×10^{-2}
^{193}At$^n \to ^{189}$Bi^p	$13/2^+ \to 13/2^+$	85	7.256	1.13×10^{-1}	1.44×10^{-1}
^{194}At$^m \to ^{190}$Bi^m	$3^+\# \to 3^+\#$	85	7.341	3.05×10^{-1}	1.13×10^{-1}
^{194}At$^n \to ^{190}$Bi^n	$(9, 10)^- \to 10^-$	85	7.329	3.97×10^{-1}	1.24×10^{-1}
^{195}At $\to ^{191}$Bi^m	$1/2^+ \to 1/2^+$	85	7.098	3.28×10^{-1}	4.83×10^{-1}
^{195}At$^m \to ^{191}$Bi^n	$7/2^- \to 7/2^-$	85	7.223	1.54×10^{-1}	1.75×10^{-1}
^{196}At $\to ^{192}$Bi	$3^+ \to 3^+$	85	7.201	2.66×10^{-1}	3.20×10^{-1}
^{197}At $\to ^{193}$Bi	$9/2^- \to 9/2^-$	85	7.104	3.50×10^{-1}	4.29×10^{-1}
^{197}At$^m \to ^{193}$Bi^m	$1/2^+ \to 1/2^+$	85	6.848	3.70×10^0	3.74×10^0
^{198}At $\to ^{194}$Bi	$3^+ \to 3^+$	85	6.894	4.67×10^0	3.86×10^0
^{198}At$^m \to ^{194}$Bi^m	$10^- \to 10^-$	85	6.997	1.19×10^0	1.60×10^0
^{199}At $\to ^{195}$Bi	$9/2^- \to 9/2^-$	85	6.780	7.81×10^0	6.34×10^0
^{200}At $\to ^{196}$Bi	$3^+ \to 3^+$	85	6.599	8.27×10^1	5.00×10^1
^{200}At$^m \to ^{196}$Bi^m	$7^+ \to 7^+$	85	6.544	1.09×10^2	8.34×10^1
^{200}At$^n \to ^{196}$Bi^n	$10^- \to 10^-$	85	6.677	6.95×10^1	2.45×10^1
^{201}At $\to ^{197}$Bi	$9/2^- \to 9/2^-$	85	6.473	1.20×10^2	9.90×10^1

α transition	$I_i^\pi \to I_j^\pi$	Z	Q_α (MeV)	$T_{1/2}^{expt}$ (s)	$T_{1/2}^{calc}$ (s)
^{202}At $\to$ ^{198}Bi	$(2,3)^+ \to (2,3)^+$	85	6.354	4.97×10^2	4.79×10^2
^{202}At^m $\to$ ^{198}Bi^m	$7^+ \to 7^+$	85	6.259	2.09×10^3	1.18×10^3
^{202}At^n $\to$ ^{198}Bi^n	$10^- \to 10^-$	85	6.353	4.79×10^2	4.84×10^2
^{203}At $\to$ ^{199}Bi	$9/2^- \to 9/2^-$	85	6.210	1.43×10^3	1.26×10^3
^{204}At $\to$ ^{200}Bi	$7^+ \to 7^+$	85	6.070	1.41×10^4	8.22×10^3
^{205}At $\to$ ^{201}Bi	$9/2^- \to 9/2^-$	85	6.020	1.61×10^4	8.52×10^3
^{206}At $\to$ ^{202}Bi^m	$5^+ \to 5^+$	85	5.815	2.13×10^5	1.20×10^5
^{207}At $\to$ ^{203}Bi	$9/2^- \to 9/2^-$	85	5.871	7.53×10^4	3.93×10^4
^{208}At $\to$ ^{204}Bi	$6^+ \to 6^+$	85	5.751	1.07×10^6	2.31×10^5
^{209}At $\to$ ^{205}Bi	$9/2^- \to 9/2^-$	85	5.757	4.75×10^5	1.33×10^5
^{195}Rn $\to$ ^{191}Po	$3/2^- \to 3/2^-$	86	7.694	6.00×10^{-3}	7.37×10^{-3}
^{195}Rn^m $\to$ ^{191}Po^m	$13/2^+ \to 13/2^+$	86	7.713	5.00×10^{-3}	6.41×10^{-3}
^{197}Rn $\to$ ^{193}Po	$3/2^- \to 3/2^-$	86	7.410	6.50×10^{-2}	7.61×10^{-2}
^{197}Rn^m $\to$ ^{193}Po^m	$13/2^+ \to 13/2^+$	86	7.509	1.90×10^{-2}	3.55×10^{-2}
^{199}Rn $\to$ ^{195}Po	$3/2^- \to 3/2^-$	86	7.132	6.28×10^{-1}	8.68×10^{-1}
^{199}Rn^m $\to$ ^{195}Po^m	$13/2^+ \to 13/2^+$	86	7.205	3.30×10^{-1}	4.77×10^{-1}
^{201}Rn $\to$ ^{197}Po	$3/2^- \to 3/2^-$	86	6.862	1.37×10^1	8.19×10^0
^{201}Rn^m $\to$ ^{197}Po^m	$13/2^+ \to 13/2^+$	86	6.911	1.12×10^1	5.33×10^0
^{203}Rn $\to$ ^{199}Po	$3/2^- \to 3/2^-$	86	6.630	6.67×10^1	6.39×10^1
^{203}Rn^m $\to$ ^{199}Po^m	$13/2^+ \to 13/2^+$	86	6.682	3.59×10^1	3.95×10^1
^{205}Rn $\to$ ^{201}Po^m	$5/2^- \to 5/2^-$	86	6.386	7.03×10^2	6.14×10^2
^{207}Rn $\to$ ^{203}Po	$5/2^- \to 5/2^-$	86	6.252	2.66×10^3	2.19×10^3
^{199}Fr $\to$ ^{195}At	$1/2^+\# \to 1/2^+$	87	7.810	1.2×10^{-2}	1.27×10^{-2}
^{200}Fr $\to$ ^{196}At	$3^+ \to 3^+$	87	7.626	4.90×10^{-2}	4.80×10^{-2}
^{201}Fr $\to$ ^{197}At	$9/2^- \to 9/2^-$	87	7.519	6.20×10^{-2}	7.83×10^{-2}
^{201}Fr^m $\to$ ^{197}At^m	$1/2^+ \to 1/2^+$	87	7.605	1.90×10^{-2}	4.06×10^{-2}
^{202}Fr $\to$ ^{198}At	$3^+ \to 3^+$	87	7.387	3.00×10^{-1}	3.38×10^{-1}
^{202}Fr^m $\to$ ^{198}At^m	$10^- \to 10^-$	87	7.381	2.90×10^{-1}	3.54×10^{-1}
^{203}Fr $\to$ ^{199}At	$9/2^- \to 9/2^-$	87	7.276	5.79×10^{-1}	6.34×10^{-1}
^{204}Fr $\to$ ^{200}At	$3^+ \to 3^+$	87	7.172	1.77×10^0	2.26×10^0
^{204}Fr^m $\to$ ^{200}At^m	$7^+ \to 7^+$	87	7.108	2.89×10^0	3.87×10^0
^{204}Fr^n $\to$ ^{200}At^n	$10^- \to 10^-$	87	7.153	2.30×10^0	2.56×10^0
^{205}Fr $\to$ ^{201}At	$9/2^- \to 9/2^-$	87	7.053	$\geqslant 3.92 \times 10^0$	4.01×10^0
^{206}Fr $\to$ ^{202}At	$(2,3)^+ \to (2,3)^+$	87	6.926	1.90×10^1	1.78×10^1
^{206}Fr^m $\to$ ^{202}At^m	$7^+ \to 7^+$	87	6.924	1.90×10^1	1.81×10^1
^{206}Fr^n $\to$ ^{202}At^n	$10^- \to 10^-$	87	7.067	1.40×10^1	5.27×10^0
^{207}Fr $\to$ ^{203}At	$9/2^- \to 9/2^-$	87	6.900	1.56×10^1	1.42×10^1
^{208}Fr $\to$ ^{204}At	$7^+ \to 7^+$	87	6.772	6.64×10^1	6.82×10^1

result, it seems that isomeric states imitate ground states to some extent, in view of the nuclear structure, considering that the preformation factor is a important resource of nuclear structure information. There are only large discrepancies in the α transitions from the g.s. of ^{185}Pb and ^{187}Pb, to the first i.s. of the corresponding daughter nuclei, which have the same angular momenta

Table 3
Same as previous tables but for numerical results above the neutron shell $N = 126$.

α transition	$I_i^\pi \to I_j^\pi$	N	Q_α (MeV)	$T_{1/2}^{expt}$ (s)	$T_{1/2}^{calc}$ (s)
$^{213}\mathrm{At} \to {}^{209}\mathrm{Bi}$	$9/2^- \to 9/2^-$	128	9.254	1.25×10^{-7}	9.87×10^{-8}
$^{215}\mathrm{Fr} \to {}^{211}\mathrm{At}$	$9/2^- \to 9/2^-$	128	9.540	8.60×10^{-8}	1.03×10^{-7}
$^{217}\mathrm{Ac} \to {}^{213}\mathrm{Fr}$	$9/2^- \to 9/2^-$	128	9.832	6.90×10^{-8}	1.01×10^{-7}
$^{219}\mathrm{Pa} \to {}^{215}\mathrm{Ac}$	$9/2^- \to 9/2^-$	128	10.080	5.30×10^{-8}	1.29×10^{-7}
$^{213}\mathrm{Po} \to {}^{209}\mathrm{Pb}$	$9/2^+ \to 9/2^+$	129	8.537	4.20×10^{-6}	2.42×10^{-6}
$^{214}\mathrm{At} \to {}^{210}\mathrm{Bi}$	$1^- \to 1^-$	129	8.987	5.58×10^{-7}	6.47×10^{-7}
$^{215}\mathrm{Rn} \to {}^{211}\mathrm{Po}$	$9/2^+ \to 9/2^+$	129	8.839	2.30×10^{-6}	2.20×10^{-6}
$^{216}\mathrm{Fr} \to {}^{212}\mathrm{At}$	$1^- \to 1^-$	129	9.174	7.37×10^{-7}	1.11×10^{-6}
$^{216}\mathrm{Fr}^m \to {}^{212}\mathrm{At}^m$	$3^- \to 3^-$	129	9.163	$< 3.55 \times 10^{-6}$	1.22×10^{-6}
$^{217}\mathrm{Ra} \to {}^{213}\mathrm{Rn}$	$9/2^+ \to 9/2^+$	129	9.161	1.60×10^{-6}	1.75×10^{-6}
$^{218}\mathrm{Ac} \to {}^{214}\mathrm{Fr}$	$1^- \to 1^-$	129	9.380	1.08×10^{-6}	1.76×10^{-6}
$^{219}\mathrm{Th} \to {}^{215}\mathrm{Ra}$	$9/2^+\# \to 9/2^+$	129	9.510	1.05×10^{-6}	1.22×10^{-6}
$^{215}\mathrm{At} \to {}^{211}\mathrm{Bi}$	$9/2^- \to 9/2^-$	130	8.178	1.00×10^{-4}	4.97×10^{-5}
$^{217}\mathrm{Fr} \to {}^{213}\mathrm{At}$	$9/2^- \to 9/2^-$	130	8.469	1.90×10^{-6}	4.06×10^{-6}
$^{219}\mathrm{Ac} \to {}^{215}\mathrm{Fr}$	$9/2^- \to 9/2^-$	130	8.830	1.18×10^{-5}	2.61×10^{-5}
$^{221}\mathrm{Pa} \to {}^{217}\mathrm{Ac}$	$9/2^- \to 9/2^-$	130	9.248	5.90×10^{-6}	1.14×10^{-5}
$^{215}\mathrm{Po} \to {}^{211}\mathrm{Pb}$	$9/2^+ \to 9/2^+$	131	7.526	1.78×10^{-3}	2.01×10^{-3}
$^{216}\mathrm{At} \to {}^{212}\mathrm{Bi}$	$1^- \to 1^-$	131	7.950	3.10×10^{-4}	3.89×10^{-4}
$^{216}\mathrm{At}^m \to {}^{212}\mathrm{Bi}^m$	$9^- \to (8^-, 9^-)$	131	8.110	1.00×10^{-4}	1.32×10^{-4}
$^{217}\mathrm{Rn} \to {}^{213}\mathrm{Po}$	$9/2^+ \to 9/2^+$	131	7.887	5.40×10^{-4}	9.37×10^{-4}
$^{218}\mathrm{Fr} \to {}^{214}\mathrm{At}$	$1^- \to 1^-$	131	8.014	1.09×10^{-3}	1.50×10^{-3}
$^{219}\mathrm{Ra} \to {}^{215}\mathrm{Rn}^m$	$7/2^+ \to 7/2^+$	131	7.821	1.51×10^{-2}	9.28×10^{-3}
$^{221}\mathrm{Th} \to {}^{217}\mathrm{Ra}^m$	$7/2^+ \to 7/2^+$	131	7.873	3.46×10^{-2}	3.93×10^{-2}

and parities with the second isomeric states (see Table 2). This may result from the effect of the shape evolution or the angular momentum hindrance (i.e. $\ell \neq 0$). The phenomenon is attractive for further investigation. Moreover, it is interesting to indicate that there are mostly α-decays from two i.s. of the same odd–odd nucleus, especially for the region around the shell $Z = 82$. This may be caused by the effect of the closed shell $Z = 82$, which provides an opportunity to check the current α-decay models strictly.

In order to obtain better insight into the agreement between theory and experiment, we plot the deviation $\log_{10}(T_{1/2}^{calc}/T_{1/2}^{expt})$ versus the neutron number of the parent nucleus for odd-A nuclei in Fig. 1, including α transitions from both the ground states and the isomeric states. Strikingly, the systematical behavior of the agreement between calculated α-decay half-lives and measured ones of different isotopic chains can reflect some information on the nuclear structure. The absolute values of deviations (see Fig. 1) are in general not larger than 0.5, which represents the values of $T_{1/2}^{calc}/T_{1/2}^{expt}$ are in the range of about 0.32–3.2. Interestingly, there is an obvious decreasing trend for the deviation as the neutron number approaching the closed shell $N = 126$, which is due to the shell effect [24]. As additional information, we have systematically investigate the exotic α-decay around the shell $N = 126$, using a Z-dependent preformation factor based on a

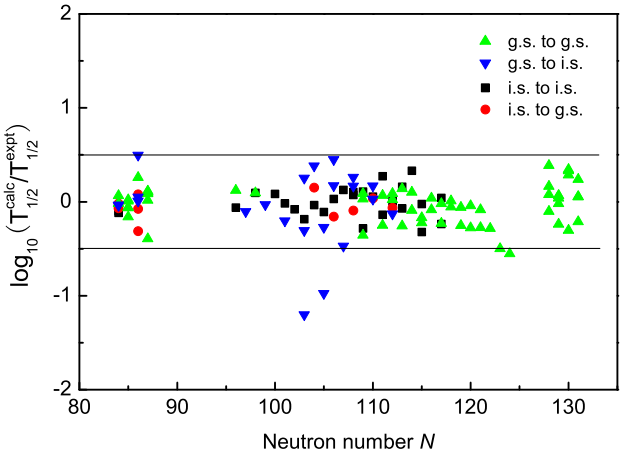

Fig. 1. The deviations between the calculated α-decay half-lives and the experimental values versus the neutron number N of the parent nucleus for odd-A nuclei. The deviation 0.5 of the decimal logarithm corresponds to the absolute one of half-lives with a factor of 3.2.

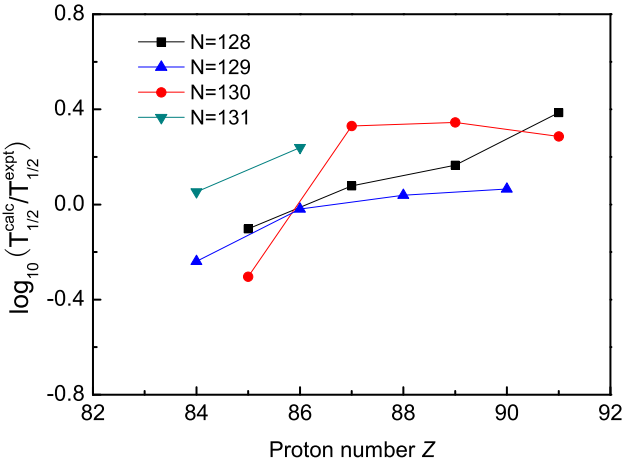

Fig. 2. The decimal logarithm of $T^{calc}_{1/2}/T^{expt}_{1/2}$ varies with the proton number for the g.s. to g.s. α transitions in different isotones above the shell closure $N = 126$.

microscopic two-level model [2]. For another illustration, deviations of calculated α-decay half-lives from experimental ones for different odd-A isotones above the shell closure $N = 126$ are shown in Fig. 2. Note that the α transitions are all from g.s. to g.s. in Fig. 2. One can see that the deviations for different isotones are in the range of -0.4–0.4, and generally increase with the proton number going away from the shell closure $Z = 82$.

To pursue further knowledge of nuclear structure properties, we also extend the present approach to the unfavored α-decays of Bi isotopes with one proton outside the shell closure. More strikingly, there are already a lot of experimental data in these isotones, including the exotic nucleus ^{209}Bi with a longest half-life in all known α-decays and an isomer ^{210}Bi^{m} with a quite long α-decay half-life. Owing to these unfavored α transitions for $Z = 83$ isotopes, the protons in-

Table 4
Calculated results of unfavored α-decays in the Bi isotopes. Different from previous tables, the third column denotes the angular momenta carried by α particles, and the extracted P_α values is added in the last column. Note that the transition $1^- \to 1^-$ is still structural hindered due to different configurations.

α transition	$I_i^\pi \to I_j^\pi$	ℓ	Q_α (MeV)	$T_{1/2}^{expt}$ (s)	$T_{1/2}^{calc}$ (s)	P_α
$^{189}\mathrm{Bi} \to {}^{185}\mathrm{Tl}$	$9/2^- \to 1/2^+$	5	7.270	1.50×10^{1}	1.63×10^{-1}	0.0108
$^{191}\mathrm{Bi} \to {}^{187}\mathrm{Tl}$	$9/2^- \to 1/2^+$	5	6.778	8.38×10^{2}	8.67×10^{0}	0.0104
$^{193}\mathrm{Bi} \to {}^{189}\mathrm{Tl}$	$9/2^- \to 1/2^+$	5	6.304	6.88×10^{4}	6.31×10^{2}	0.0092
$^{195}\mathrm{Bi} \to {}^{191}\mathrm{Tl}$	$9/2^- \to 1/2^+$	5	5.832	6.78×10^{6}	7.68×10^{4}	0.0113
$^{209}\mathrm{Bi} \to {}^{205}\mathrm{Tl}$	$9/2^- \to 1/2^+$	5	3.137	6.00×10^{26}	1.22×10^{25}	0.0203
$^{211}\mathrm{Bi} \to {}^{207}\mathrm{Tl}$	$9/2^- \to 1/2^+$	5	6.750	1.54×10^{2}	3.04×10^{0}	0.0197
$^{213}\mathrm{Bi} \to {}^{209}\mathrm{Tl}$	$9/2^- \to 1/2^+$	5	5.982	1.41×10^{5}	4.49×10^{3}	0.0318
$^{210}\mathrm{Bi} \to {}^{206}\mathrm{Tl}^m$	$1^- \to 2^-$	2	4.785	8.20×10^{11}	1.62×10^{9}	0.0020
$^{210}\mathrm{Bi} \to {}^{206}\mathrm{Tl}^n$	$1^- \to 1^-$	0	4.746	5.47×10^{11}	1.51×10^{9}	0.0028
$^{210}\mathrm{Bi}^m \to {}^{206}\mathrm{Tl}^m$	$9^- \to 2^-$	8	5.042	1.74×10^{14}	4.06×10^{10}	2.33×10^{-4}
$^{210}\mathrm{Bi}^m \to {}^{206}\mathrm{Tl}^n$	$9^- \to 1^-$	8	5.004	2.43×10^{14}	7.82×10^{10}	3.22×10^{-4}

volved in the α-particle formation should be from two major shells. Hence the overlap, between the actual wave function of the parent nucleus and that of the corresponding decaying-state describing the cluster coupled to the daughter nucleus, is quite small [2]. With these in mind, we predict that the α-preformation factor is obviously smaller than the usual chosen value. The formation factor can be extracted as the ratio of the calculated half-life (assuming $P_\alpha = 1$ firstly) to the experimental value [39]. The detailed results are given in Table 4, whose first two columns are the same with the previous tables. The third column indicates the angular momentum carried by the α particle. Experimental Q_α values and half-lives are listed in fourth and fifth columns, respectively. The last two columns denote the calculated half-lives and the extracted P_α values. Here the angular momentum carried by the α particle is taken as the minimum value obeying the spin–parity selection rule. Indeed, P_α values of unfavored α transitions are obviously much smaller than those of favored transitions for these Bi isotopes. The reason is that these unfavored transitions involve unpaired nucleons to enter into the formation of α particles. The small P_α values for odd-A Bi isotopes, in general, vary smoothly versus the neutron number of parent nuclei. Moreover, the P_α values of the parent nuclei above the closed shell $N = 126$ are just slightly larger than those of other odd-A isotopes, which may be due to the shell effect [24]. The above two phenomena may conclude that the small P_α value mainly result from the effect of the unpaired proton involved in the formation of the α particle. As additional information, the effect of neutron shell $N = 126$ on decay energies is clear. The Q_α value of ^{209}Bi is obviously smaller as compared with that of other isotope, as displayed in Table 4.

Because of the block effect of the unpaired neutron, the P_α values of ^{210}Bi or $^{210}\mathrm{Bi}^m$ are clearly smaller than those of the odd-A isotopes (see Table 4). For odd–odd nuclei, their spins and parities are mostly assigned tentatively based on systematics and indirect evidence from α-decay studies [47,48]. ^{210}Bi, with one proton and one neutron outside the double magic shell, has been paid special attention in theoretical studies [52,53]. Its ground state and 9^- isomeric state are considered as multiplet of the configuration $(\pi h_{9/2})(\upsilon g_{9/2})$, and the configurations of the corresponding daughter nucleus are $(\pi d_{3/2})^{-1}(\upsilon p_{1/2})^{-1}$ and $(\pi s_{1/2})^{-1}(\upsilon p_{1/2})^{-1}$, respectively, for the 2^- isomeric state and 1^- isomeric state. Hence the α transition to the 2^- isomeric state involves the paired proton in the $d_{3/2}$ level, while the transition to 1^- state involves the paired

proton in the $s_{1/2}$ level. Based on the shell-model picture, the $s_{1/2}$ orbit is just above the former orbit. This indicates that it is more difficult for the proton in the $d_{3/2}$ orbit to form the α particle. Consequently, the P_α value of the transition to 2^- is slightly smaller than that of the transition to 1^- for ^{210}Bi or ^{210}Bi^m, as shown in Table 4. Note that the configurations are actually different for the parent and daughter nucleus in the transition $1^- \to 1^-$ of ^{210}Bi, resulting in the structural hindrance (unfavored α-decay). Moreover, based on the above analysis of the configuration, two neutrons involved in the α-particle formation are from two major shells for ^{210}Bi. This can be considered as another reason causing that P_α values of this odd–odd nucleus are smaller than other odd-A Bi isotopes. Actually, the situation is even more complicated due to the proton–neutron coupling for the case of odd–odd nuclei. This is worth further investigation.

To measure the goodness of the agreement between our overall calculations and the experimental data, the standard deviation is introduced, which is defined as $\sqrt{\langle\sigma^2\rangle} = \sqrt{\frac{1}{N}\sum_{i=1}^{N}(\log_{10} T^i_{calc} - \log_{10} T^i_{expt})^2}$. Its value is 0.24 for the favored α transitions of exotic nuclei near the shell closure $N = 82$, 126 and $Z = 82$, which indicates the agreement, including some new data, is generally within a factor of 2. This means that the present approach called the MTPA for deformed nuclei, well reproduces the experimental α-decay half-lives of both odd-A and odd–odd nuclei, and is also valid for both ground and isomeric states. Combining with our previous work, the modified two-potential approach within the cluster model can give a reasonable description of α-decay.

4. Summary

To conclude, we have used the modified two-potential approach for deformed nuclei to give a systematic investigation on the favored α-decays near the closed shell region, no matter what it concerns ground states or isomeric states. The double-folded nuclear and Coulomb potentials, taking into account the deformation effect, are numerically constructed to obtain the α-decay width. As shown in Tables 1, 2, and 3, the calculated α-decay half-lives are in good agreement with the measured values for ground and isomeric states of both odd-A and odd–odd nuclei. This denotes that these α transitions, from ground states and isomeric states, can be described well by means of the modified two-potential approach within the cluster model. Moreover, the shell effect on α transitions is discussed to some extent. We also extend the study to the unfavored transitions of the Bi isotones, to pursue some further knowledge of nuclear structure properties. The present work is helpful for the future study on the expected α transitions in the ground and isomeric states near the neutron shell $N = 126$ and the next proton and neutron shell closures.

Acknowledgements

This work is supported by the National Natural Science Foundation of China (Grant Nos. 11035001, 10735010, and 10975072), by the 973 National Major State Basic Research and Development of China (Grant Nos. 2007CB815004 and 2010CB327803), by CAS Knowledge Innovation Project No. KJCX2-SW-N02, and by Research Fund of Doctoral Point (RFDP), Grant No. 20100091110028.

References

[1] E. Rutherford, H. Geiger, Proc. R. Soc. 81 (1908) 162.

[2] Z. Ren, G. Xu, Phys. Rev. C 36 (1987) 456;
Z. Ren, G. Xu, Phys. Rev. C 38 (1988) 1078.
[3] H. Horiuchi, Nucl. Phys. A 522 (1991) 257.
[4] J. Wauters, N. Bijnens, P. Dendooven, M. Huyse, Han Yull Hwang, G. Reusen, J. von Schwarzenberg, Phys. Rev. Lett. 72 (1994) 1329.
[5] R.G. Lovas, R.J. Liotta, A. Insolia, K. Varga, D.S. Delion, Phys. Rep. 294 (1998) 265.
[6] P.E. Hodgson, E. Běták, Phys. Rep. 374 (2003) 1.
[7] A.P. Leppänen, et al., Phys. Rev. C 75 (2007) 054307.
[8] S. Hofmann, G. Münzenberg, Rev. Mod. Phys. 72 (2000) 733.
[9] T.N. Ginter, et al., Phys. Rev. C 67 (2003) 064609.
[10] Yu.Ts. Oganessian, et al., Phys. Rev. C 72 (2005) 034611;
Yu.Ts. Oganessian, et al., Phys. Rev. C 74 (2006) 044602.
[11] Yu.Ts. Oganessian, et al., Phys. Rev. Lett. 104 (2010) 142502.
[12] G. Gamow, Z. Phys. 51 (1928) 204.
[13] E.U. Condon, R.W. Gurney, Nature 122 (1928) 439.
[14] G. Royer, J. Phys. G: Nucl. Part. Phys. 26 (2000) 1149.
[15] J. Dong, H. Zhang, Y. Wang, W. Zuo, J. Li, Nucl. Phys. A 832 (2010) 198.
[16] D. Ni, Z. Ren, J. Phys. G: Nucl. Part. Phys. 37 (2010) 035104;
D. Ni, Z. Ren, J. Phys. G: Nucl. Part. Phys. 37 (2010) 105107.
[17] C. Xu, Z. Ren, Phys. Rev. C 73 (2006) 041301(R);
C. Xu, Z. Ren, Phys. Rev. C 74 (2006) 014304.
[18] V.Yu. Denisov, A.A. Khudenko, Phys. Rev. C 80 (2009) 034603.
[19] K.P. Santhosh, George Joseph Jayesh, Sabina Sahadevan, Phys. Rev. C 82 (2010) 064605.
[20] D.S. Delion, S. Peltonen, J. Suhonen, Phys. Rev. C 73 (2006) 014315.
[21] S. Peltonen, D.S. Delion, J. Suhonen, Phys. Rev. C 75 (2007) 054301.
[22] D. Ni, Z. Ren, Phys. Rev. C 81 (2010) 024315.
[23] D. Ni, Z. Ren, T. Dong, C. Xu, Phys. Rev. C 78 (2008) 044310.
[24] C. Qi, A.N. Andreyev, M. Huyse, R.J. Liotta, P. Van Duppen, R.A. Wyss, Phys. Rev. C 81 (2010) 064319.
[25] D.S. Delion, Phys. Rev. C 80 (2009) 024310.
[26] G. Royer, Nucl. Phys. A 848 (2010) 279.
[27] V.Yu. Denisov, A.A. Khudenko, Phys. Rev. C 79 (2009) 054614;
V.Yu. Denisov, A.A. Khudenko, Phys. Rev. C 82 (2010) 059901, Erratum.
[28] C. Xu, Z. Ren, Phys. Rev. C 78 (2008) 057302.
[29] R.D. Page, et al., Phys. Rev. C 53 (1996) 660.
[30] T. Bäck, et al., Eur. Phys. J. A 16 (2003) 489.
[31] E. Coenen, K. Deneffe, M. Huyse, P. Van Duppen, J.L. Wood, Phys. Rev. Lett. 54 (1985) 1783.
[32] J. Wauters, P. Dendooven, M. Huyse, G. Reusen, P. Van Duppen, Phys. Rev. C 47 (1993) 1447.
[33] A.N. Andreyev, et al., Phys. Rev. C 79 (2009) 064320;
A.N. Andreyev, et al., Phys. Rev. C 80 (2009) 024302.
[34] A.N. Andreyev, et al., Phys. Rev. C 80 (2009) 054322;
A.N. Andreyev, et al., J. Phys. G: Nucl. Part. Phys. 37 (2010) 035102.
[35] G.G. Adamian, N.V. Antonenko, W. Scheid, A.S. Zubov, Phys. Rev. C 78 (2008) 044605.
[36] S.A. Gurvitz, G. Kalbermann, Phys. Rev. Lett. 59 (1987) 262.
[37] S.A. Gurvitz, P.B. Semmes, W. Nazarewicz, T. Vertse, Phys. Rev. A 69 (2004) 042705.
[38] Y. Qian, Z. Ren, Nucl. Phys. A 852 (2011) 82.
[39] Y. Qian, Z. Ren, D. Ni, J. Phys. G: Nucl. Part. Phys. 38 (2011) 015102.
[40] Y. Qian, Z. Ren, D. Ni, Phys. Rev. C 83 (2011) 044317.
[41] K. Wildermuth, Y.C. Tang, A Unified Theory of the Nucleus, Academic Press, New York, 1997.
[42] G.R. Satchler, W.G. Love, Phys. Rep. 55 (1979) 183.
[43] A.M. Kobos, B.A. Brown, P.E. Hodgson, G.R. Satchler, A. Budzanowski, Nucl. Phys. A 384 (1982) 65.
[44] T.L. Stewart, M.W. Kermode, D.J. Beachey, N. Rowley, I.S. Grant, A.T. Kruppa, Nucl. Phys. A 611 (1996) 332.
[45] D.S. Delion, A. Sandulescu, W. Greiner, Phys. Rev. C 69 (2004) 044318.
[46] K. Varga, R.G. Lovas, R.J. Liotta, Phys. Rev. Lett. 69 (1992) 37.
[47] G. Audi, O. Bersillon, J. Blachot, A.H. Wapstra, Nucl. Phys. A 729 (2003) 3.
[48] NNDC of the Brookhaven National Laboratory, http://www.nndc.bnl.gov.
[49] K. Van de Vel, et al., Phys. Rev. C 68 (2003) 054311.

[50] A.N. Andreyev, et al., Phys. Rev. C 73 (2006) 044324.
[51] P. Möller, J.R. Nix, W.D. Myers, W.J. Swiatecki, At. Data Nucl. Data Tables 59 (1995) 185.
[52] L. Coraggio, A. Covello, A. Gargano, N. Itaco, Phys. Rev. C 76 (2007) 061303.
[53] P. Alexa, J. Kvasil, N.V. Minh, R.K. Sheline, Phys. Rev. C 55 (1997) 179.